Modeling of Eddy-Current Loss of Electrical Machines and Transformers Operated by Pulsewidth-Modulated Inverters

Ruifang Liu[1,2], Chris Chunting Mi[2], and David Wenzhong Gao[3]

[1]Beijing Jiaotong University, Beijing 100044, China
[2]Department of Electrical and Computer Engineering, University of Michigan, Dearborn, MI 48128 USA
[3]Department of Electrical and Computer Engineering, Tennessee Tech University, Cookeville, TN 38505 USA

Pulsewidth-modulated (PWM) inverters are used more and more to operate electrical machines and to interface renewable energy systems with the utility grid. However, there are abundant high-frequency harmonics in the output voltage of a PWM inverter, which increase the iron losses and result in derating of the machine or transformer connected to them. Predicting the iron losses caused by the PWM supply is critical for the design of electrical machines and transformers operated by PWM inverters. These losses are primarily attributed to eddy-current loss caused by the PWM supply. In this paper, after analyzing the harmonic components of PWM voltage, we derive the effects of different parameters of PWM switching on the eddy-current loss. We compare the iron losses modeled with the proposed analytical methods on a three-phase transformer, a dc motor, and an induction motor with the results of time-stepping finite-element analysis and experiments. We provide detailed equations for the prediction of iron losses. These equations can be directly applied in the design and control of PWM converters and electric motors to improve energy efficiency in electrical machines and transformers operated from PWM converters.

Index Terms—**Amplitude modulation ratio, core loss, eddy-current loss, iron loss, PWM inverter, switching frequency.**

I. Introduction

In industrial applications, speed regulation of electric motors is often necessary. An economic solution is to use ac motors supplied with variable voltage variable frequency (VVVF) inverters, commonly known as frequency converters. Other important applications of frequency converters are found in power systems to realize flexible ac transmission, to interface renewable energy systems with the utility grid, or to be used as power factor correction devices. Pulsewidth modulation (PWM) voltage control is widely utilized in modern power converters. The high-frequency harmonics in the output voltage induce additional losses in the electric machines or transformers operated from PWM converters. In-depth understanding of PWM loss mechanism is important for predicting iron losses and improving energy efficiency in electrical machines and transformers. Prediction of iron losses of motors supplied by PWM converters is usually studied through finite-element analysis (FEA) or modified equivalent circuit. Some preliminary work was carried out on induction motors, permanent-magnet synchronous motors, and switched reluctance motors [1]–[7]. These studies are mainly focused on the variation of iron losses in different parts of the motor taking into account the influence of PWM supply. The effects of different parameters of PWM supply on iron losses have not been discussed. In [8]–[12], some valuable experiments were carried out to measure iron losses of wound cores and motors under different PWM parameters, such as amplitude modulation ratio and switching frequency. Some useful conclusions were obtained. The experiment shows that the heavy iron loss increases in the case of PWM supply is mainly attributed to the eddy-current loss increment inside the iron core [13]. However, the theoretical analysis on the effect of PWM parameters on iron losses still has not been studied. In this paper, after analyzing the amplitude of harmonics of the output voltage of PWM converters, the eddy-current loss is derived as a function of the modulation index, switching frequency, and dc link voltage.

Since time-stepping FEA can accurately predict iron losses with nonlinear B–H characteristic of the iron [14], [15], the time-stepping FEA is also adopted in this paper to calculate the eddy-current loss on a single phase transformer to gain further confidence of the analytical results. Experiments are conducted to validate theoretical analysis.

II. Analysis of Voltage Harmonics of PWM Supply

The general principle of bipolar PWM is shown in Fig. 1, where the triangle waveform (carrier, $V_{\rm tri}$) of switching frequency f_c is compared with the control signal ($V_{\rm control}$) of frequency f_1. The intersections between the two waveforms determine the switching points of power devices. The ratio between switching frequency f_c and fundamental frequency f_1 is defined as frequency modulation ratio $m_f, m_f = f_c/f_1$. The ratio between the amplitude of the control waveform $V_{\rm control}$ and that of the triangle waveform $V_{\rm tri}$ is defined as amplitude modulation ratio $m_a, m_a = V_{\rm control}/V_{\rm tri}$.

There are many different methods to determine the switching points, such as natural sampling rule, regular sampling, and selected harmonic elimination rule.

The symmetrical regular sampling rule is a basic method in sampling. The switch points can be determined from Fig. 1 for this sampling method:

$$\alpha_k = \frac{\pi}{2m_f}\left\{2k-1+(-1)^k m_a \sin\left[(k+m)\frac{\pi}{m_f}\right]\right\} \quad k=1,\ldots,2m_f$$
$$\text{when } (-1)^k = 1, m=-1; \quad \text{when } (-1)^k=-1, m=0 \quad (1)$$

where α_k is the switching point.

The output voltage of inverter contains the fundamental voltage and other high-frequency harmonic contents. The

Digital Object Identifier 10.1109/TMAG.2008.923537

Color versions of one or more of the figures in this paper are available online at http://ieeexplore.ieee.org.

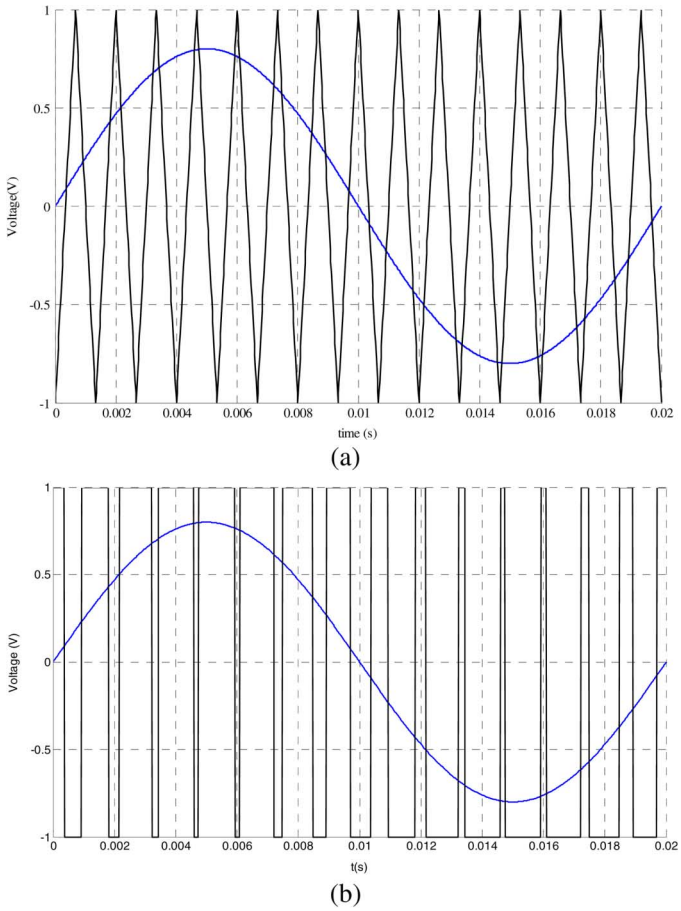

Fig. 1. Principle of bipolar PWM ($m_a = 0.8, m_f = 15, f_1 = 50$ Hz). (a) Carrier waveform $V_{\rm tri}$ and control waveform $V_{\rm control}$. (b) PWM output and its fundamental component.

general Fourier series of the output voltage can be given as the following:

$$v(t) = \sum_{n=1}^{\infty} v_n(t) = \sum_{n=1}^{\infty} (a_n \cos n\omega t + b_n \sin n\omega t) = \sum_{n=1}^{\infty} V_n \sin(n\omega t + \varphi_n) \tag{2}$$

where ω is the fundamental angular frequency, n is the order of harmonics, V_n is the amplitude of the nth harmonic, a_n and b_n are the Fourier coefficients, φ_n is the phase angle of the nth harmonic, and

$$a_n = \frac{V_{\rm dc}}{n\pi} \sum_{k=1}^{2m_f} (-1)^k \sin(n\alpha_k) \tag{3}$$

$$b_n = \frac{V_{\rm dc}}{n\pi} \sum_{k=1}^{2m_f} (-1)^k \cos(n\alpha_k) \tag{4}$$

$$V_n = \sqrt{a_n^2 + b_n^2} = \frac{V_{\rm dc}}{n\pi} \sqrt{\left[\sum_{k=1}^{2R} (-1)^k \cos(n\alpha_k)\right]^2 + \left[\sum_{k=1}^{2R} (-1)^{k+1} \sin(n\alpha_k)\right]^2} \tag{5}$$

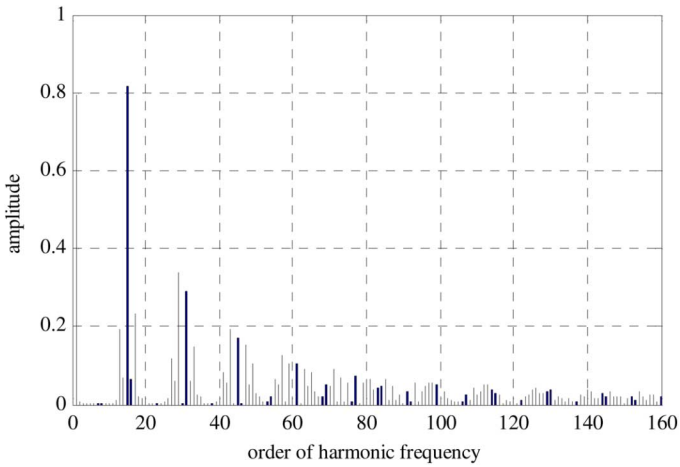

Fig. 2. Harmonic frequency analysis of output voltage.

$$\varphi_n = \tan^{-1}\left(\frac{b_n}{a_n}\right) \tag{6}$$

where $V_{\rm dc}$ is the dc link voltage.

According to (5), the amplitude of the harmonics is dependent on the dc link voltage $V_{\rm dc}$, the order of the harmonic waveform n, and the switching points α_k. The switching points α_k is determined by frequency modulation ratio m_f and amplitude modulation ratio m_a as shown in (1). Fig. 2 shows the harmonic spectrum of the PWM output waveform for $m_f = 15$ and $m_a = 0.8$. The PWM output waveform contains carrier frequency-related harmonics with modulation frequency-related sidebands in the form of $mf_c \pm nf_1$, where m and n are integers and $m + n$ is an odd integer.

III. Analytical Calculation of Eddy-Current Loss

The total iron loss density $p_{\rm iron}$ is commonly expressed in the following form for sinusoidal varying magnetic flux density B with angular frequency ω [14], [15]

$$p_{\rm iron} = p_h + p_c = k_h B^{\beta}\omega + k_c B^2 \omega^2 \ ({\rm W/m^3}) \tag{7}$$

where p_h and p_c are the hysteresis loss density and the classical eddy-current loss density, respectively; k_h and k_c are the hysteresis and eddy-current constants, respectively; and β is the Steinmetz constant, all of which depend on the lamination material. Because the heavy iron loss increase in the case of PWM supply is mainly induced by the eddy-current loss increment [13], this paper will focus on the analysis of the eddy-current loss.

Equation (7) is only valid for flux density under sinusoidal time-varying condition. Under PWM supply, there are many high-frequency harmonic flux density components. Under the assumption of linear material, the flux density harmonic amplitude is proportional to the voltage harmonic amplitude. So the harmonic components of the PWM voltage output can be analyzed, and the eddy-current loss of each harmonic component can be calculated. Although such assumption is not in accordance with the magnetic property of the core material, considering that the objective of this work is to compare the iron losses influenced by different parameters of PWM supply, the absolute error caused by the assumption does not affect the final results.

In order to give a clear view of the iron losses associated with the PWM parameters, a single phase transformer was used as a first example. Under secondary winding open circuit condition, the primary circuit equation is

$$v(t) = e(t) + i(t)R + L_\sigma \frac{di(t)}{dt} \tag{8}$$

where $v(t)$ is the applied voltage, $e(t)$ is the back electromotive force, $i(t)$ is the current, L_σ is the leakage inductance of the primary winding, and R is the resistance of the primary winding.

When neglecting the voltage drop on winding resistor R and leakage inductance L_σ

$$v(t) \approx e(t) = N_1 \frac{d\Phi(t)}{dt} = N_1 A \frac{dB(t)}{dt} \tag{9}$$

where N_1 is the number of turns of the primary winding, and A is the cross section area of the transformer core. Substitute (2) into (9), under linear material assumption, the flux density is

$$B(t) = -\sum_{n=1}^{\infty} B_n \cos(n\omega t + \varphi_n) \tag{10}$$

where B_n is the flux density of the nth harmonic

$$B_n = \frac{V_n}{N_1 A n \omega}. \tag{11}$$

The eddy-current loss can be obtained as

$$\begin{aligned} p_c &= \sum_{n=1}^{\infty} p_{c,n} = \sum_{n=1}^{\infty} k_c B_n^2 (n\omega)^2 \\ &= \sum_{n=1}^{\infty} k_c \left(-\frac{V_n}{N_1 A n \omega}\right)^2 (n\omega)^2 = \frac{k_c}{(N_1 A)^2} \sum_{n=1}^{\infty} (V_n)^2. \end{aligned} \tag{12}$$

Combining (5) and (12), the eddy-current losses can be derived as

$$\begin{aligned} p_c = \frac{k_c}{(N_1 A \pi)^2} \sum_{n=1}^{\infty} \left(\frac{V_{\rm dc}}{n}\right)^2 \Bigg\{ \left[\sum_{k=1}^{2R} (-1)^k \cos(n\alpha_k)\right]^2 \\ + \left[\sum_{k=1}^{2R} (-1)^k \sin(n\alpha_k)\right]^2 \Bigg\} \end{aligned} \tag{13}$$

$$\begin{aligned} p_c = K \sum_{n=1}^{\infty} \left(\frac{V_{\rm dc}}{n}\right)^2 \Bigg\{ \left[\sum_{k=1}^{2R} (-1)^k \cos(n\alpha_k)\right]^2 \\ + \left[\sum_{k=1}^{2R} (-1)^k \sin(n\alpha_k)\right]^2 \Bigg\} \end{aligned} \tag{14}$$

where

$$K = \frac{k_c}{(N_1 A \pi)^2}.$$

From the above equations, it can be concluded that the eddy-current loss is related to the amplitude of the fundamental and other high-order harmonics. Furthermore, it is related to the switching points α_k and dc link voltage $V_{\rm dc}$. Switching point α_k is related to the sampling method of switching points. If the regular sampling method is adopted, α_k is determined by the frequency modulation ratio and the amplitude modulation ratio according to (1). Each harmonic component will contribute to the total eddy-current loss. According to Fig. 2, the fundamental voltage and the harmonics at the switching frequency contribute more to the eddy-current loss.

TABLE I
SPECIFICATIONS OF THE TRANSFORMER

Power	1 kW
Voltage	110 V/55V
N_1/N_2	150/75
Cross section area	2048 mm^2

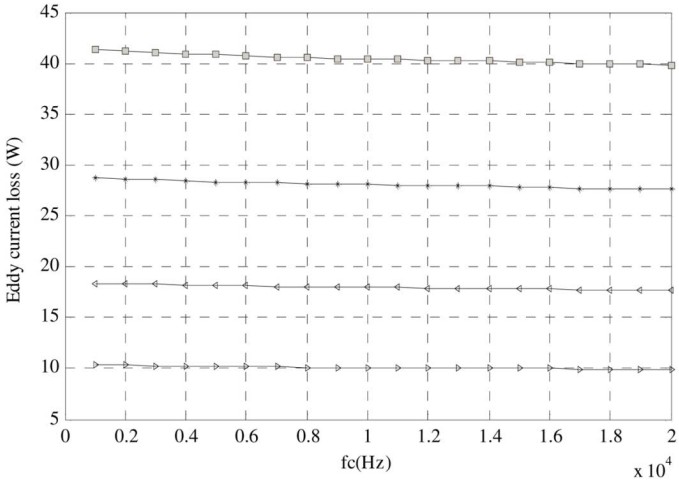

Fig. 3. Eddy-current loss versus switching frequency. From top to bottom: $V_1 = 1.2, 1.0, 0.8, 0.6$ per unit, respectively.

IV. EFFECTS OF PWM PARAMETERS ON THE EDDY-CURRENT LOSS

A. Effect of Switching Frequency

Using the above analysis, the effect of different PWM parameters on eddy-current loss is studied for a single phase transformer. The specifications of the transformer are shown in Table I. Eddy-current loss constant is $k_c = 0.07$ [14], [15].

In order to find the influence of switching frequency on the eddy-current loss, a constant amplitude modulation ratio $m_a = 0.9$ is used. The fundamental frequency is $f_1 = 50$ Hz, and switching frequency varies from 1 to 20 kHz. The losses have been calculated at different dc link voltage. Under linear assumption, the amplitude of the fundamental flux density is directly proportional to the amplitude of the fundamental voltage. The regulation of the amplitude of fundamental voltage is achieved by adjusting the dc link voltage. Fig. 3 shows the eddy-current loss variation with different switching frequencies, where V_1 indicates the per unit value of the amplitude of the fundamental voltage.

Only a small decrease of eddy-current loss is observed in Fig. 3 when the switching frequency increases. The loss is almost constant when changing switching frequency at a given fundamental voltage. According to (12), the eddy-current loss is mainly related to the amplitude of the fundamental voltage

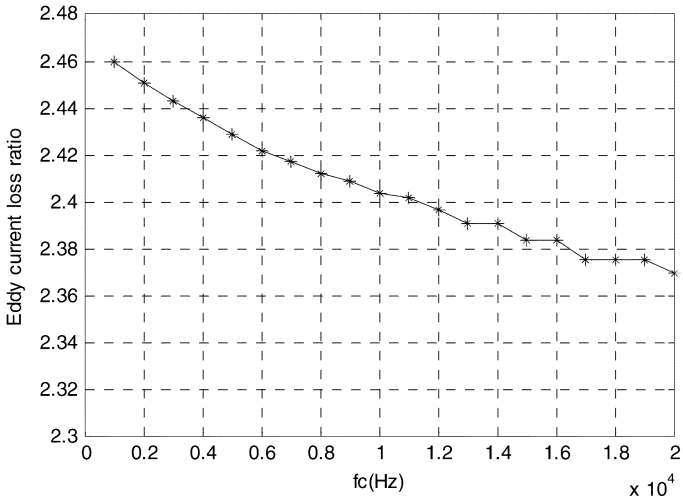

Fig. 4. Eddy-current loss ratio versus switching frequency at $m_a = 0.9$.

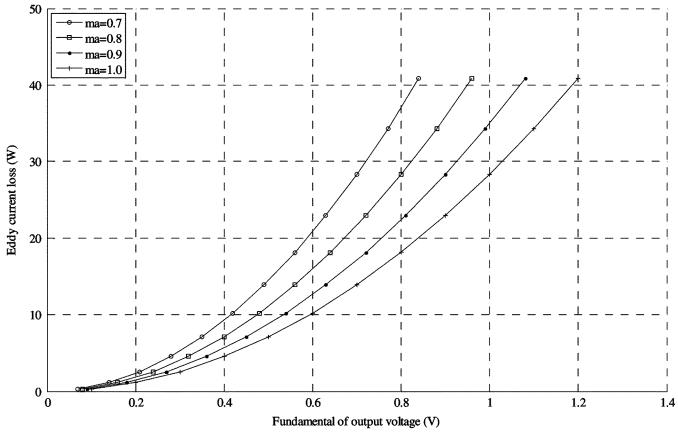

Fig. 5. Effect of amplitude modulation ratio on eddy-current loss.

and the amplitude of the harmonic voltage at the switching frequency.

In order to compare the increment of eddy-current loss under PWM supply, the concept "*loss ratio*" is introduced. The *loss ratio* is defined as the eddy-current loss under PWM supply compared to the eddy-current loss with pure sinusoidal voltage supply. Fig. 4 shows that the *loss ratio* varies with switching frequency. The calculation results are the same when changing the dc link voltage. From Fig. 4 it can be seen that the *loss ratio* at 1 kHz is 2.46 times the loss if the supply voltage is pure sinusoidal wave at fundamental frequency. When the switching frequency increases to 20 kHz the *loss ratio* decreases to 2.37. There is only 3.7% loss drop. It can be concluded that the effect of switching frequency on the eddy-current loss is negligible. This conclusion is validated by experimental results [9].

B. Effect of Amplitude Modulation Ratio

In order to find the effect of amplitude modulation ratio on the eddy-current loss, a constant fundamental frequency of $f_1 = 50$ Hz and constant switching frequency $f_c = 5$ kHz is used. The dc link voltage changes from 0.1 V_{DCN} to 1.2 V_{DCN}, where V_{DCN} is the rated dc link voltage. The eddy-current losses are calculated under different amplitude modulation ratio $m_a = 0.7, 0.8, 0.9, 1.0$. Fig. 5 shows the eddy-current losses varying

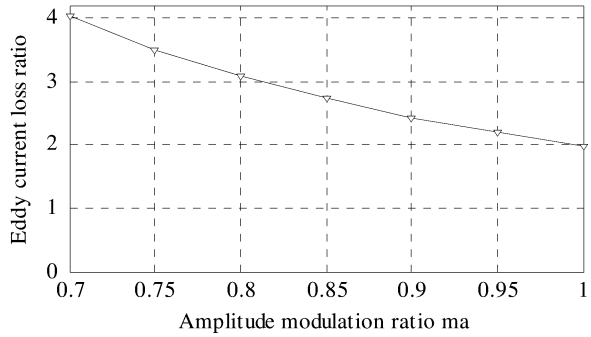

Fig. 6. Effect of amplitude modulation ratio on eddy-current loss ratio.

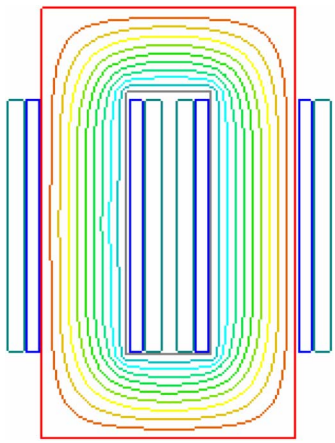

Fig. 7. Flux linkage distribution of the transformer.

with the fundamental voltage in per unit value. Fig. 6 shows the eddy-current *loss ratio* between PWM supply and pure sinusoidal supply, for different amplitude modulation ratio. The results indicate that the eddy-current loss drops with the increase of amplitude modulation ratio m_a. The reason is that at a higher amplitude modulation ratio the amplitude of harmonic components becomes relatively low. Therefore, the eddy-current loss will decrease with the amplitude modulation ratio. To reduce the iron losses when adopting a PWM inverter, a high amplitude modulation ratio is recommended. In this case, the dc link voltage needs to vary with the output voltage [10].

V. Comparison of FEA and Analytical Results

In order to verify the analytical calculation results, the time-stepping FEA is used to validate the calculations in this research. FEA can take into account the nonlinear magnetic property of the core. The circuit equation is given by (8).

The input voltage of the primary winding is a time-varying quantity as shown in (2). The time stepping FEA is carried out with the Maxwell 3D software by Ansoft. Fig. 7 shows the cross sectional flux distribution of the transformer at one time step.

When the calculation enters into the steady state, the eddy-current loss $p_c(t)$ can be obtained. The average power loss within one fundamental period is easily obtained by

$$P_c = \frac{1}{T}\int_{t_0}^{t_0+T} p_c(t)dt. \tag{15}$$

In order to compare with the analytical method, FEA calculations are carried out under pure sinusoidal wave supply

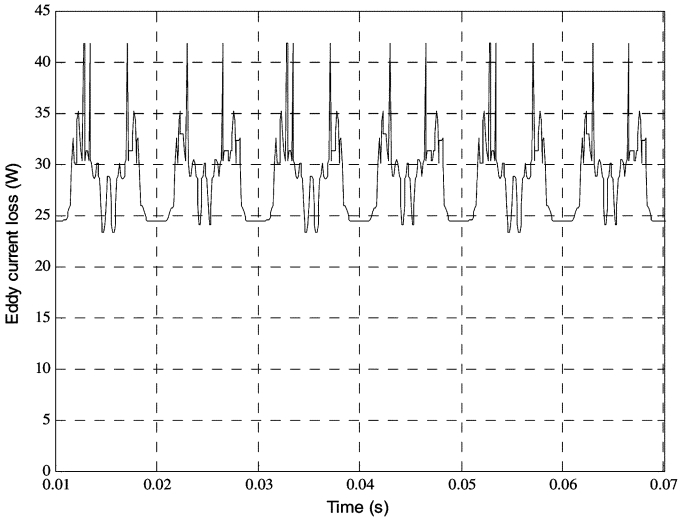

Fig. 8. Eddy-current loss waveform under PWM supply.

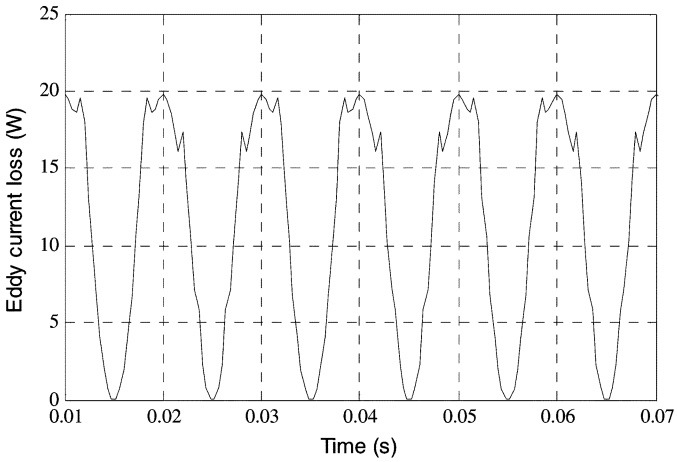

Fig. 9. Eddy-current loss waveform under sine wave supply.

and under PWM supply, respectively. The calculations under PWM supply are carried out with different parameters such as switching frequency, amplitude modulation ratio, and dc link voltage.

Fig. 8 shows the waveform of the eddy-current loss supplied with a PWM inverter, at $f_c = 1$ kHz and $f_1 = 50$ Hz, $m_a = 0.9$, $V_{\rm dc} = 1.0V_{\rm dcN}$. The average eddy-current loss is 28.45 W. Fig. 9 shows the waveform of the eddy-current loss when supplied with pure sine waveform at $f_1 = 50$ Hz, $V_m = 0.9V_{\rm dcN}$. The average loss is 11.23 W. In the above two conditions, the fundamental voltage of the transformer is the same. The eddy-current loss under PWM supply is 2.53 times that under pure sine wave supply.

Table II compares the analytical and FEM results in the above two conditions. Table III compares the FEA results and the analytical results for the effect of amplitude modulation ratio on the eddy-current loss.

It can be seen from Table II and Table III that the eddy-current loss calculated by FEA and the analytical method are slightly different. However, the iron *loss ratio* is very close between FEA and analytical results. The reason of the discrepancy of loss data

TABLE II
EDDY-CURRENT LOSS COMPARISON BETWEEN ANALYTICAL AND FEA CALCULATION

	Analytical	FEA
$P_{\rm c}$ (W) sine wave supply	11.67	11.23
$P_{\rm c}$ (W) PWM supply	28.70	28.45
Ratio	2.46	2.53

TABLE III
EDDY-CURRENT LOSS RATIO COMPARISON OF PWM AND SINE WAVE SUPPLY

M	0.7	0.8	0.9	1.0
Analytical	4.07	3.11	2.46	1.99
FEA	3.92	3.12	2.53	1.92
Error (%)	3.83	0.32	2.76	3.65

by the two methods is caused by the assumption in the analytical method where uniform distribution of magnetic flux and linear core material property are assumed. The error between the two methods on eddy-current *loss ratio* is less than 4%. It therefore validated the analytical method.

VI. EDDY-CURRENT LOSS OF DC MOTORS WITH PWM SUPPLY

PWM supply is widely used in the speed control of dc motors. The pulsation components in the PWM supply will also induce additional losses. The losses induced by PWM supply include copper loss, hysteresis loss, and eddy-current loss. Among them, eddy-current loss is the dominating loss mechanism according to theoretical research and experiments carried out in the past [18]–[21]. In [18], it presented a valuable approach to estimate motor PWM losses. It is composed of normalized PWM loss evaluation and PWM loss characterization experiment for a maximal loss point. Under qualitative analysis, the normalized eddy-current loss variation with the duty cycle of PWM was obtained. However, there is a lack of theoretical support in the study. In this paper, based on the Fourier series analysis of the PWM waveform, the eddy-current loss is calculated under linear material assumption. The effect of duty cycle on PWM eddy-current loss is analyzed.

A. Fourier Analysis of the PWM Supply of a DC Motor

Instantaneous normalized PWM voltage of one PWM period is shown in Fig. 10, where D is the duty cycle of the PWM waveform, $V_{\rm dc}$ is the dc supply voltage, and T is the switching period. The average dc output voltage is $DV_{\rm dc}$, which is proportional to the PWM duty cycle. The pulsation component is responsible for the additional losses caused by PWM.

In one period, the Fourier series of the PWM voltage is as follows:

$$v(t) = V_0 + \sum_{n=1}^{\infty} V_n \sin(n\omega_s t + \varphi_n) \tag{16}$$

where ω_s is the switching frequency, and

$$V_0 = DV_{\rm dc} \tag{17}$$

$$V_n = \frac{V_{\rm dc}}{n\pi}\cos(nD\pi). \tag{18}$$

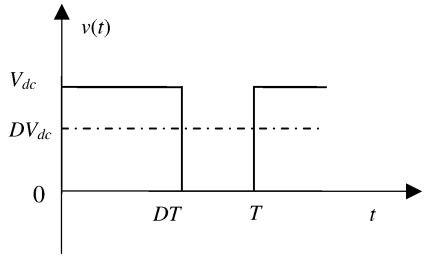

Fig. 10. Instantaneous voltage in one PWM period.

B. Eddy-Current Loss Analysis

In general, the iron losses of dc motor should be calculated according to the magnetic flux density in the teeth and yoke separately. In this paper, only the influence of PWM parameter on the losses is of interest. So the teeth and yoke are assumed to have the same and uniform flux density. To determine the dc component of the PWM voltage, neglecting the armature resistance R_a, the voltage equation of a dc motor is

$$V_0 = E + IR_a \approx E = K_E \Phi \omega_r = K_E B_0 A \omega_r \tag{19}$$

where ω_r is the rotor speed, K_E is the electromotive force constant, and

$$B_0 = \frac{V_0}{K_E A \omega_r} = \frac{DV_{\rm dc}}{K_E A \omega_r}. \tag{20}$$

For the pulsation component of the PWM voltage, under linear material assumption, the voltage equation can be derived as

$$\begin{aligned} \sum_{n=1}^{\infty} V_n \sin(n\omega t + \varphi_n) &= K_E \frac{d\Phi}{dt} + iR_a \\ &\approx K_E \frac{d\Phi}{dt} = K_E \frac{d[(B(t)A]}{dt} \\ \therefore B(t) &= -\frac{1}{K_E A} \sum_{n=1}^{\infty} \frac{V_n}{n\omega_s} \cos(n\omega_s t + \varphi_n) \\ &= -\sum_{n=1}^{\infty} B_n \cos(n\omega_s t + \varphi_n) \end{aligned} \tag{21}$$

where

$$B_n = \frac{V_n}{n\omega_s A K_E} = \frac{\cos(nD\pi) V_{\rm dc}}{n\omega_s A K_E n\pi}. \tag{22}$$

When the rotor is rotating, the magnetic field in the teeth and yoke will alternate. Both B_0 and $B_{\rm n}$ will induce eddy-current loss in the rotor cores. The eddy-current loss induced by B_0 is

$$P_{\rm dc} = k_c B_0^2 \omega_s^2 = k_c \left(\frac{DV_{\rm dc}}{K_E A \omega_s} \right)^2 \omega_s^2 = KD^2 \tag{23}$$

where

$$K = k_c \left(\frac{V_{\rm dc}}{K_E A} \right)^2.$$

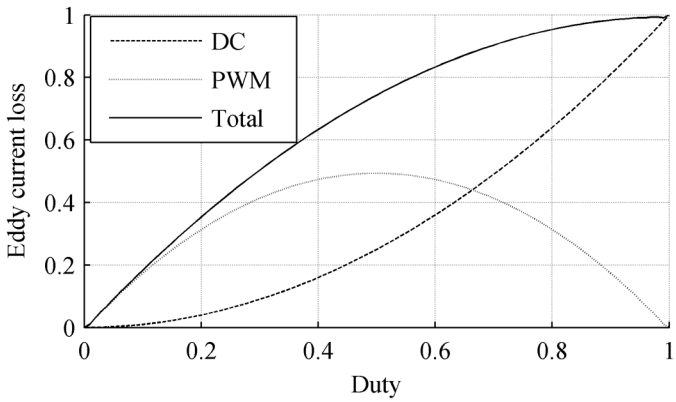

Fig. 11. Eddy-current loss of dc motor supplied by PWM converter.

The eddy-current losses induced by the pulsation components are

$$\begin{aligned} P_{\rm PWM} &= \sum_{n=1}^{\infty} k_c B_n^2 (n\omega_s)^2 \\ &= \sum_{n=1}^{\infty} k_c \left[\frac{\cos(n\pi D) V_{\rm dc}}{K_E S n \omega_s n\pi} \right]^2 (n\omega_s)^2 = K \sum_{n=1}^{\infty} \left[\frac{\cos(n\pi D)}{n\pi} \right]^2. \end{aligned} \tag{24}$$

The total eddy-current losses are

$$P_{\rm Total} = P_{\rm dc} + P_{\rm PWM}. \tag{25}$$

Assume a constant dc link voltage $V_{\rm dc}$, while changing the duty cycle from 0 to 1, the output voltage will increase from 0 to $V_{\rm dc}$. Using the above equations, the relationship of the eddy-current loss as a function of duty cycle can be obtained, as shown in Fig. 11. It can be seen that at $D = 0.5$, the eddy-current loss caused by the harmonics of the PWM supply reaches its extreme. The result is validated by measurements [18]. The total eddy-current losses will achieve maximal value at $D = 1$.

VII. Experimental Validation

In order to validate the theoretical analysis, experiments were performed on a three-phase autotransformer, a dc motor, and an induction motor.

A. Transformer Testing

The test transformer is an autotransformer. A Yokogawa PZ400 Power Analyzer is used to measure the input power of the transformer under no-load condition. Under the same fundamental voltage, the difference between the input power of PWM supply and pure sinusoidal supply can be treated as the extra loss induced by the PWM inverter. This extra loss includes iron losses and copper loss due to PWM supply. Since the copper loss under no-load condition is negligible, the extra loss is mainly the iron loss caused by the PWM supply.

Fig. 12 shows the comparison of measurement and calculated data with respect to the effect of switching frequency on PWM iron losses. The test is taken under constant fundamental voltage of 80 V. It can be seen that there is a small decrease in measured

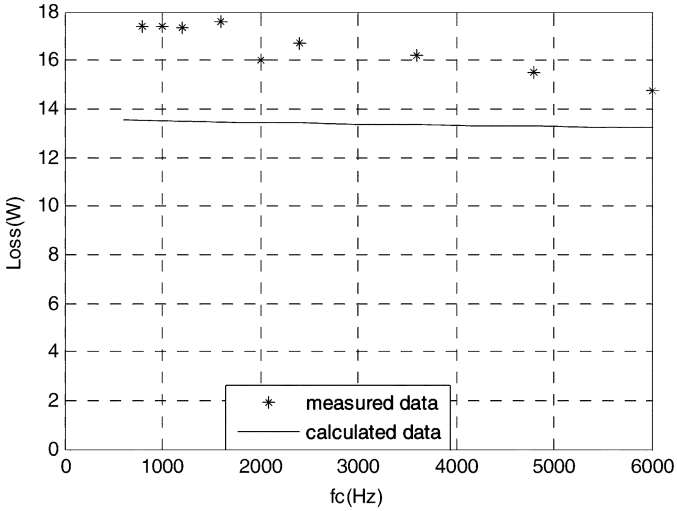

Fig. 12. Effect of switching frequency on transformer PWM iron losses.

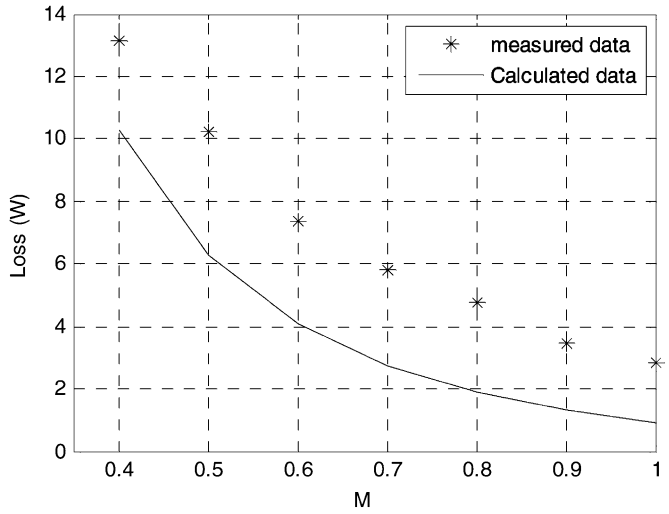

Fig. 13. Effect of amplitude modulation ratio on PWM iron losses of transformer.

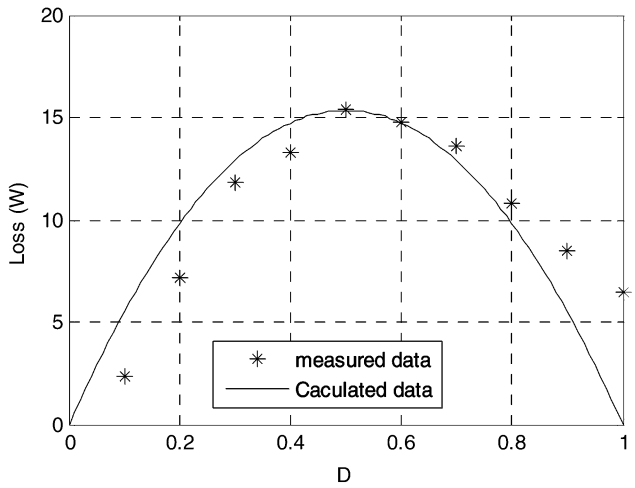

Fig. 14. Effect of duty ratio on dc motor PWM iron losses under constant dc bus link voltage 100 V.

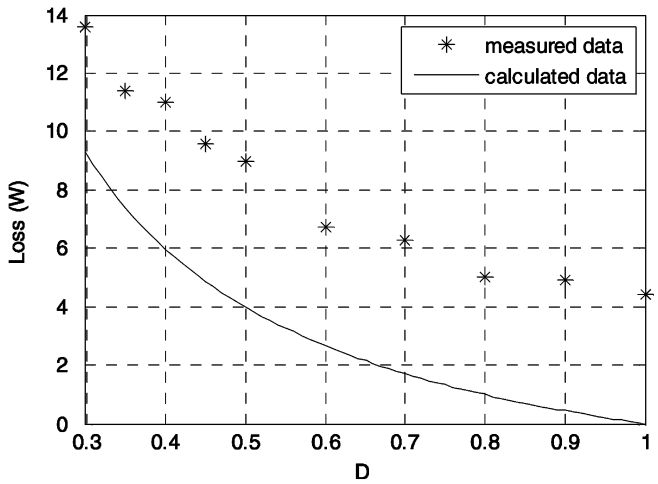

Fig. 15. Effect of duty ratio on PWM iron losses under constant rotation speed.

loss with the increase of the switching frequency. But the decrease is not significant. Fig. 13 shows the effect of amplitude modulation ratio on PWM iron losses for measured and calculated data. With the increase of amplitude modulation ratio, the PWM iron losses will decrease. Both the measured value and the calculated value have the same variation trend.

In Figs. 12 and 13, there is a discrepancy between the calculated results and the measured results. The reason is that the measured losses include hysteresis loss, eddy-current loss, and copper loss due to PWM supply. But in the measured data, it is not easy to separate eddy-current loss from other losses. Therefore, the measured PWM loss is generally greater than the calculated PWM iron losses.

B. DC Motor Testing

The experiment on a dc motor is also under no-load condition. The dc motor is rated at 125 V, 2 kW. The dc motor is tested with pure dc power supply, as well as a full bridge dc–dc converter. The difference between the input power of the dc motor under PWM supply and under pure dc power supply is considered as the loss induced by PWM converter. Fig. 14 shows the loss variation with duty cycle at constant dc bus voltage of 100 V. The calculated and measured iron losses are consistent and in both measurement and calculations, the eddy-current losses reach the maximum value at 0.5 duty ratio.

In order to study the effect of duty ratio on PWM loss under the same rotation speed, the output dc voltage of PWM converter is kept constant and the dc bus voltage is adjusted according to the duty ratio. Fig. 15 shows the relationship of PWM loss versus duty ratio at constant speed of 396 rpm. It can be seen that from both measured and calculated losses, the extra PWM iron losses decrease with the increase of duty ratio. Therefore, in order to minimize eddy-current loss in dc machines, it is beneficial to maintain a large duty ratio by varying the dc link voltage to achieve the desired speed.

The discrepancy shown in Fig. 15 is believed to be attributed by the exclusion of effects of PWM supply on hysteresis loss and copper loss in the calculations, which are included in the measurements.

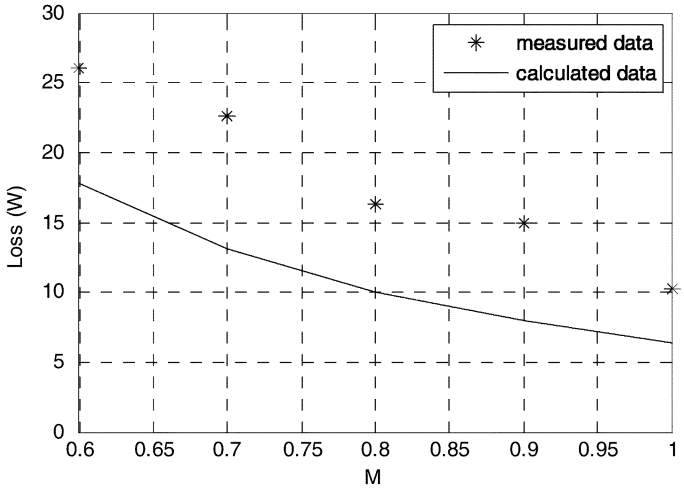

Fig. 16. Effect of amplitude modulation ratio on PWM iron losses of induction motor at 80 V.

C. Induction Motor Testing

The induction motor is a wound rotor machine rated at 2 kW, 208 V. Under the same fundamental voltage, the dc bus link voltage is adjusted. The measured PWM losses at different amplitude modulation ratios are shown in Fig. 16, together with the calculation results. It shows that with the increase of amplitude modulation ratio, the PWM losses will decrease. Again, the trend of the measured data matches that of the calculated data.

VIII. Conclusion

This paper presented the effects of the parameters of PWM supply on the eddy-current loss of electric machines and transformers operated by PWM converters. The eddy-current loss caused by PWM supply is studied for a transformer, an induction motor, and a dc motor. For sinusoidal PWM power supply, the results show that switching frequency has little effects on the eddy-current loss. The amplitude modulation ratio plays an important role in the eddy-current loss. In dc motors, the eddy-current loss reaches maximum for $D = 0.5$ and in this case, the PWM harmonics contributes 50% to the total eddy-current loss. The overall increase of eddy-current loss due to the existence of voltage harmonics are significant when compared to electric systems supplied from a pure sinusoidal or pure dc power source. The results are validated by FEA and experiments on an autotransformer, a dc motor, and an induction motor.

Due to the limitation of the laboratories, it was not possible to extract eddy-current loss data from the total iron loss measurement in the testing. Nonetheless, the test results presented in this paper confirms that the additional losses caused by PWM supply in transformers and electric machines are not negligible. Therefore, additional studies and experiments are necessary to further quantitatively study the PWM loss. It is also important to study the PWM loss when the machines or transformers work under loaded conditions. This will be our future work.

Acknowledgment

The authors would like to thank the support of Ansoft Corporation who provided the Maxwell 2D and 3D software for this study.

References

[1] J. J. Lee, Y. K. Kim, and H. Nam, "Loss distribution of three-phase induction motor fed by pulsewidth-modulated inverter," *IEEE Trans. Magn.*, vol. 40, no. 2, pp. 762–765, Mar. 2004.
[2] E. N. Hildebrand and H. Roehrdanz, "Losses in three-phase induction machines fed by PWM converter," *IEEE Trans. Energy Convers.*, vol. 16, no. 3, pp. 228–233, Sep. 2001.
[3] P. J. Leonard, P. Marketos, A. J. Moses, and M. Lu, "Iron losses under PWM excitation using a dynamic hysteresis model and finite elements," *IEEE Trans. Magn.*, vol. 42, no. 4, pp. 907–910, Apr. 2006.
[4] T. H. Kim and J. Lee, "Comparison of the iron loss of a flux-reversal machine under four different PWM modes," *IEEE Trans. Magn.*, vol. 43, no. 4, pp. 1725–1728, Apr. 2007.
[5] H. Toda, K. Senda, and M. Ishida, "Effect of material properties on motor iron loss in PM brushless DC motor," *IEEE Trans. Magn.*, vol. 41, no. 10, pp. 3937–3939, Oct. 2005.
[6] J. Sagarduy, A. J. Moses, and F. J. Anayi, "Current losses in electrical steels subjected to matrix and classical PWM excitation waveforms," *IEEE Trans. Magn.*, vol. 42, no. 10, pp. 2818–2820, Oct. 2006.
[7] K. Yamazaki and Y. Seto, "Iron loss analysis of interior permanent-magnet synchronous motors-variation of main loss factors due to driving condition," *IEEE Trans. Ind. Appl.*, vol. 42, no. 4, pp. 1045–1052, Jul./Aug. 2006.
[8] A. Boglietti, A. Cavagnino, T. L. Mthombeni, and P. Pillay, "Comparison of lamination iron losses supplied by PWM voltages: US and European experiences," in *Proc. IEEE Int. Electr. Machines Drives Conf.*, May 2005, pp. 1431–1436.
[9] A. Boglietti, P. Ferraris, M. Lazzari, and M. Pastorelli, "Change of the iron losses with the switching supply frequency in soft magnetic materials supplied by PWM inverter," *IEEE Trans. Magn.*, vol. 31, no. 6, pp. 4250–4252, Nov. 1995.
[10] A. Boglietti, P. Ferraris, M. Lazzari, and F. Profumo, "Effects of different modulation index on the iron losses in soft magnetic materials supplied by PWM inverter," *IEEE Trans. Magn.*, vol. 29, no. 6, pp. 3234–3236, Nov. 1993.
[11] T. Lotten, M. P. Pillay, and N. A. Singampalli, "Lamination core loss measurements in machines operating with PWM or non-sinusoidal excitation," in *Proc. Electr. Machines Drives Conf.*, Jun. 1–4, 2003, vol. 2, pp. 743–746.
[12] F. Sixdenier, L. Morel, and J. P. Masson, "Introducing dynamic behavior of magnetic materials into a model of a switched reluctance motor drive," *IEEE Trans. Magn.*, vol. 42, no. 3, pp. 398–404, Mar. 2006.
[13] A. Boglietti, P. Ferraris, M. Lazzari, and F. Profumo, "Iron losses in magnetic materials with six-step and PWM inverter supply," *IEEE Trans. Magn*, vol. 27, no. 6, pp. 5334–5336, Nov. 1991.
[14] C. Mi, G. R. Slemon, and R. Bonert, "Modeling of iron losses of permanent-magnet synchronous motors," *IEEE Trans. Ind. Appl.*, vol. 39, no. 3, pp. 734–742, May 2003.
[15] W. Roshen, "Iron loss model for permanent-magnet synchronous motors," *IEEE Trans. Magn.*, vol. 43, no. 8, pp. 3428–3434, Aug. 2007.
[16] H. Kaimori, A. Kameari, and K. Fujiwara, "FEM computation of magnetic field and iron loss in laminated iron core using homogenization method," *IEEE Trans. Magn.*, vol. 43, no. 4, pp. 1405–1408, Apr. 2007.
[17] K. B. Jang, T. H. Kim, Y.-D. Chun, and J. Lee, "Iron loss calculation in a flux-concentration-type LOA," *IEEE Trans. Magn.*, vol. 41, no. 10, pp. 4024–4026, Oct. 2005.
[18] A. Ruderman, "Electrical machine PWM loss evaluation basics," in *Energy Efficiency in Motor Driven Systems*, Heidelberg, Germany, Sep. 5–8, 2005.
[19] M. K. Jamil and N. A. Demerdash, "Harmonics and core losses of permanent magnet DC motors controlled by chopper circuits," *IEEE Trans. Energy Convers.*, vol. 5, no. 2, pp. 408–414, Jun. 1990.
[20] M. K. Jamil and N. A. Demerdash, "Effects of chopper control circuits on core losses of permanent magnet DC motors," *IEEE Trans. Magn.*, vol. 25, no. 5, pp. 3572–3574, Sep. 1989.
[21] A. Boglietti, P. Ferraris, M. Lazzari, and M. Pastorelli, "About the possibility of defining a standard method for iron loss measurement in soft magnetic materials with inverter supply," *IEEE Trans. Ind. Appl.*, vol. 33, no. 5, pp. 1283–1288, Sep. 1997.

Manuscript received October 24, 2007; revised April 9, 2008. Corresponding author: C. Mi (e-mail: chrismi@umich.edu).